

# Chapter 4

## Spatial Distribution of Pulsars

### 4.1 Introduction

If massive OB stars are the progenitors of pulsars, then the death rate of massive OB stars must match the birth rate of pulsars. Blaauw, in his work in 1985, addressed the question that if the death rate of OB stars match the birth rate of pulsars. He restricted his analysis to the solar neighbourhood since the observational selection effects can be ignored. With the knowledge of the average age of pulsars and the number of pulsars in the solar neighbourhood, he estimated the local birth rate of pulsars to be about  $24 \text{ Myr}^{-1} \text{ kpc}^{-1}$ . With the assumption that the local population of pulsars is produced by the local massive star population, he estimated the death rate of local OB stars. It turned out that the death rate of massive stars can account for only about 15% of the birth rate of pulsars. With this knowledge he advanced a hypothesis that the vast majority of pulsars must be produced by relatively low mass stars of mass  $6\text{--}10M_{\odot}$ . This led him to conclude that pulsars are, on the Galactic scale, tracers of past locations of spiral arms, rather than the present locations of spiral arms.

The aim of the work described in this chapter is to find out if there exists a correlation between the Galactic distribution of pulsars and the expected loca-

tion of spiral arms at different epochs. Looking for such a correlation is quite important, for it gives an independent estimate of a few important quantities like the masses of progenitors of pulsars, pulsar velocities, etc.

The threshold mass for neutron star formation has been estimated by many theoretical studies. The overall picture from these studies can be summarised as follows. For stars in the mass range  $8M_{\odot}$  to  $\sim 10M_{\odot}$  the O-Ne-Mg core becomes degenerate. With this degenerate core, the threshold for electron capture may be crossed after further fuel ignition. This causes the onset of core collapse, since the electron degeneracy pressure decreases as electrons are removed (Hillebrandt 1987). For stars with masses  $> 10M_{\odot}$ , an iron core of mass  $> 1.2M_{\odot}$  is formed, which collapses as a consequence of iron-helium transition (Hillebrandt 1987). Thus, for masses  $\gtrsim 8M_{\odot}$ , stars are expected to leave neutron star remnants.

The correlation analysis which is described in this chapter provides an independent method to estimate the threshold mass for neutron star formation based on the spatial distribution of pulsars in the Galaxy.

## 4.2 Selection Effects

Figure 4.1 gives the distribution of observed population of pulsars in the Galaxy, superimposed on the electron density distribution map (Taylor & Cordes 1993). The location of the Sun in this figure is (0,8.5). The concentration of pulsars to the solar neighbourhood is obviously due to observational selection effects. If one wants to get an estimate of the global distribution of pulsars, the effect due to selection effects must be removed. As mentioned in chapter 2, the detectability of a pulsar is affected by both its luminosity and its pulsed nature. The interstellar scattering and dispersion result in the broadening of the observed pulses, reducing the peak pulsed flux. The effect of such selection effects can be readily seen in

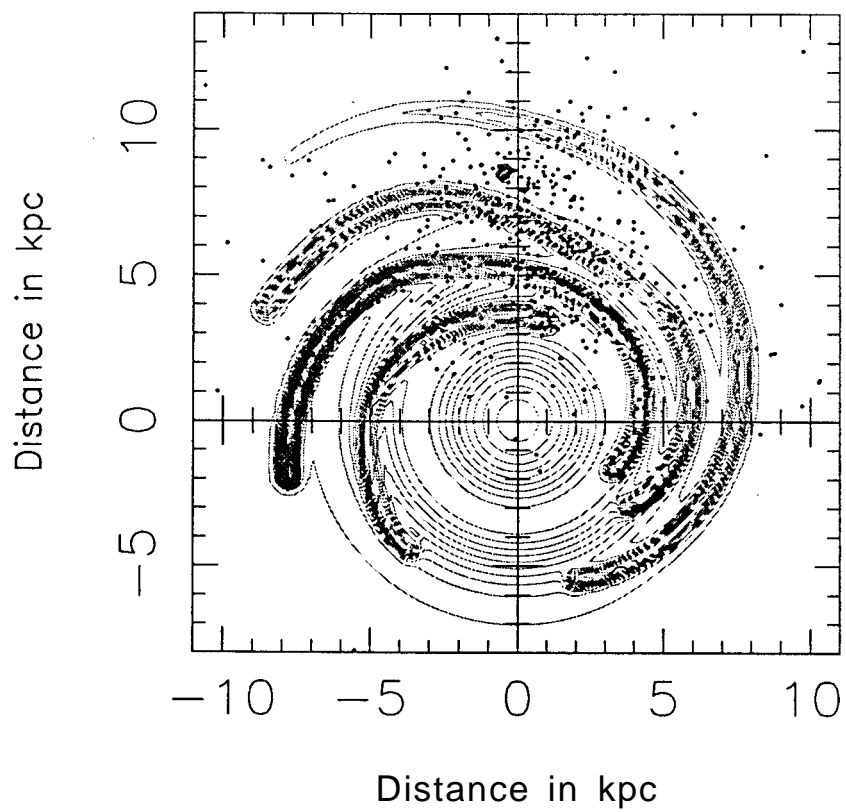


Figure 4.1: The electron density distribution in the Galaxy by Taylor & Cordes (1993). Projected locations of all pulsars are plotted as dots. The Sun is at (0,8.5).

figure 4.2, where the distribution of minimum distances ( $d_{\min}$ ) from the nearest arm to the pulsars is plotted. The value of  $d_{\min}$  is taken to be positive when it refers to the side of the arm which is nearer to the Sun and as negative otherwise. One expects this distribution to be symmetric if the selection effects are not significant. In reality the probability of detection reduces as the distance from the Sun increases. Hence, pulsars closer to the Sun (which are assigned positive  $d_{\min}$  values) tend to skew the distribution of minimum distances. The feature at  $d_{\min} \approx 0.9$  kpc can be attributed to the bias caused by the pulsars close to the Sun. This figure stresses the need to compensate for the selection effects.

The following section describes the procedure which we have adopted to compensate for the selection effects as a function of the position in the Galaxy. For this work, only those pulsars which are in principle "detectable" by any one of the eight major surveys mentioned in chapter 2, are considered. They are about 325 in number.

### 4.2.1 Scale Factors as a Function of the Position in the Galaxy

A complete treatment of modelling various selection effects is described in chapter 2 (for original references, see Narayan 1987; Narayan & Ostriker 1990). As described in chapter 2 the scale factor is defined as the ratio of the true number of pulsars in the Galaxy to the observed number. Therefore, the true number of pulsars in a bin of width  $\Delta P$  around the period  $P$  and  $\Delta B$  around the field  $B$  can be given by (equation 2.8 in chapter 2),

$$N_{\text{true}}(P, B) = \sum_{i=1}^{N_{\text{psr}}} S_i(P, B)$$

where  $N_{\text{psr}}$  is the total number of known pulsars in the bin. Here,  $N_{\text{true}}(P, B)$  can be regarded as a probability distribution for the occurrence of  $P$  and  $B$ .

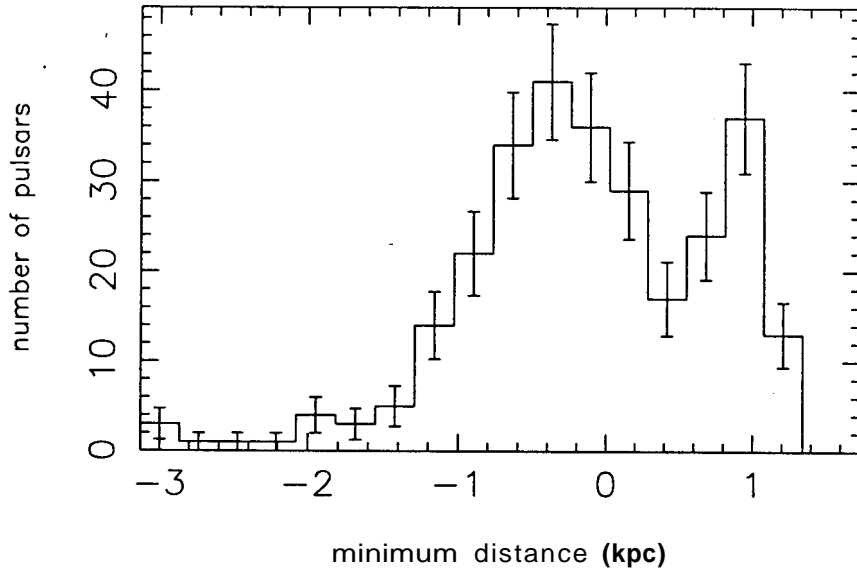


Figure 4.2: Distribution of minimum distances ( $d_{\min}$ ) of pulsars to the nearest spiral arm. The value of  $d_{\min}$  is taken to be positive when it is from that side of the arm which is nearer to the Sun, and as negative otherwise. The peak at 0.9 kpc is identified to be due to the pulsars in the solar neighbourhood. Error bars indicate 1  $\sigma$  deviation on either side.

Figure 2.6 of chapter 2 gives the distribution of the true number of pulsars as a function of **B** and **P**. This map was used to compute the scale factors as a function of position in the Galaxy. The procedure can be briefly described as follows. Given the location of a pulsar in the Galaxy (from the selected sample set) pulsars of various periods and fields were populated in that location, with the weightage given by the above equation. The reciprocal of the fraction of pulsars detectable by at least one of the eight surveys was taken as the *scale factor corresponding to that location*. Since one is interested in only the projected distribution of pulsars in the Galactic plane, the  $z$  dependence was averaged over as given below.

$$S(R, \phi) = \alpha \left[ \int_{-z_{\max}}^{z_{\max}} \frac{\exp(-|z|/z_o)}{S(R, z, \phi)} dz \right]^{-1} \quad (4.1)$$

where  $\alpha = \int_{-z_{\max}}^{z_{\max}} \exp(-|z|/z_o) dz$ , and  $z_o$  and  $z_{\max}$  are taken to be 0.45 kpc and 2.5 kpc. The scale factors thus computed range between 1 to about 6000, with 90% of the samples having scale factors less than 500. The large values of scale factors can be in error by a large factor, for in such cases the pulsars are situated in the inner region of the Galaxy where modelling of the selection effects is not very satisfactory. *Hence, all pulsars with scale factors above 500 were neglected.* This automatically excludes pulsars within a galactocentric radius of  $R = 4$  kpc, where the spiral arms are poorly defined. Figure 4.3 shows the distribution of these scale factors.

### 4.3 Correlation between the pulsar distribution and the spiral arms

The scale factors as described in the last section help to compensate for the observational selection effects. They can be visualised as *weighting factors* for

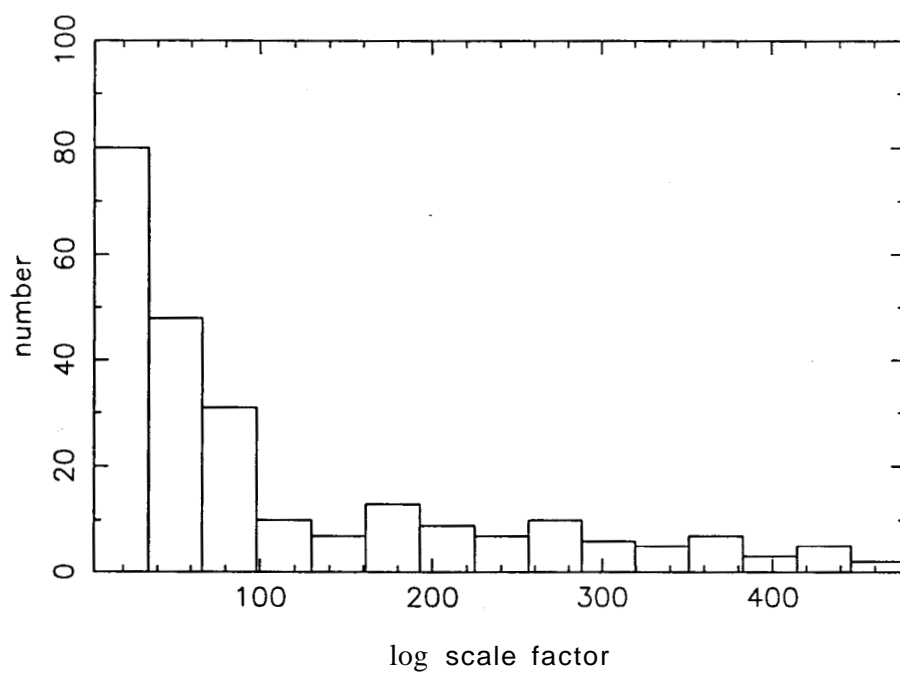


Figure 4.3: Distribution of scale factors of the known pulsars. As described in section 4.2.1 these scale factors are position dependent.

various locations in the Galaxy. With the help of these weighting factors one constructs the *true* distribution of pulsars in the Galaxy. What we would like to do is to look for a correlation between the distribution of pulsars and the spiral pattern of the Galaxy, with the help of this true distribution of pulsars. This section describes the procedure adopted to look for such a correlation.

The matter in the Galaxy does not rotate like a rigid pattern. Deduced from observations, the tangential velocity of rotation about the centre of the Galaxy remains constant for a large range of galactocentric radii (from about 4–5 kpc to about 17–20 kpc). However, the spiral pattern in the Galaxy rotates around the galactic centre like a rigid pattern. The relative galactocentric angular motion between the matter in the Galaxy and the spiral density wave pattern is given by (see Lin et al. 1969),

$$\beta(t, R) = V_{\text{rot}} \left( \frac{1}{R} - \frac{1}{R_c} \right) t \quad (4.2)$$

where  $R_c$  is the corotation resonance radius of the Galaxy, and  $V_{\text{rot}}$  is the velocity in the model of the Galaxy with a flat rotation curve. The value of this velocity was assumed to be 225 km/sec., as recommended by the IAU (Kerr and Lynden-Bell 1986). At the corotation resonance radius, the circular velocity of the Galaxy and the velocity of the spiral pattern are equal. Matter leads the spiral pattern inside the corotation radius, and the pattern leads the matter outside  $R_c$ . This relation enables one to calculate the location of pulsars with respect to the spiral pattern at any epoch (with the present epoch being taken as the reference). If pulsars had no spatial velocities, then their present locations should correlate with the mass distribution at the epoch of the formation of their progenitors. However, such a correlation is expected to be smeared out due to. (1) the spread of the birth places of the progenitors. and (2) the velocity of the progenitors. The star



forming regions in the Galaxy are expected to be confined to within a belt along the spiral arms of width  $\approx 100$  pc. As the progenitors have typical velocities of about 10 km/sec. (see Gies & Bolton 1986; Lequeux 1979), this would cause a smearing of about a few hundreds of parsecs in space. Therefore, one can afford to neglect the above mentioned two effects.

To get an idea of the mass distribution along the spiral arms, it is assumed that the mass distribution is adequately described by the arm component of the electron density model due to Taylor and Cordes (1993). As this electron density model is based on the observations of giant HII regions in the Galaxy, this assumption may be justified (see Taylor & Cordes 1993; Georgelin & Georgelin 1976; Caswell & Haynes 1987 for details). Also, the value of the corotation resonance radius of the Galaxy was assumed to be 14 kpc, since this value seems to fit the HI data rather well (Burton 1971). Given these assumptions one can define the correlation between the pulsar distribution and the spiral pattern as,

$$C(t) = \frac{\sum_{i=1}^{N_{\text{psr}}} S(R_i, \phi_i) n(R_i, \phi_i - \beta(t, R_i))}{\sum_{i=1}^{N_{\text{psr}}} S(R_i, \phi_i)} \quad (4.3)$$

where,  $n$  is the mass density at the extrapolated location of  $i^{\text{th}}$  pulsar and  $S(R_i, \phi_i)$  is the corresponding scale factor. The mass distribution perpendicular to the spiral arm in this model is a Gaussian, with  $a = 0.3$  kpc. This correlation is computed for a given relative epoch and corotation resonance radius, by rotating the pulsar distribution relative to the spiral pattern as per equation 4.2. The variation of the correlation as a function of the relative epoch (with respect to the present epoch) for an assumed value of 14 kpc (see section 4.3.3) to the corotation radius is given in figure 4.4. This plot shows a peak correlation at an epoch corresponding to about 60 Myr ago., accompanied by another peak at the present epoch. The peak at  $-60$  Myr can be associated with the past positions

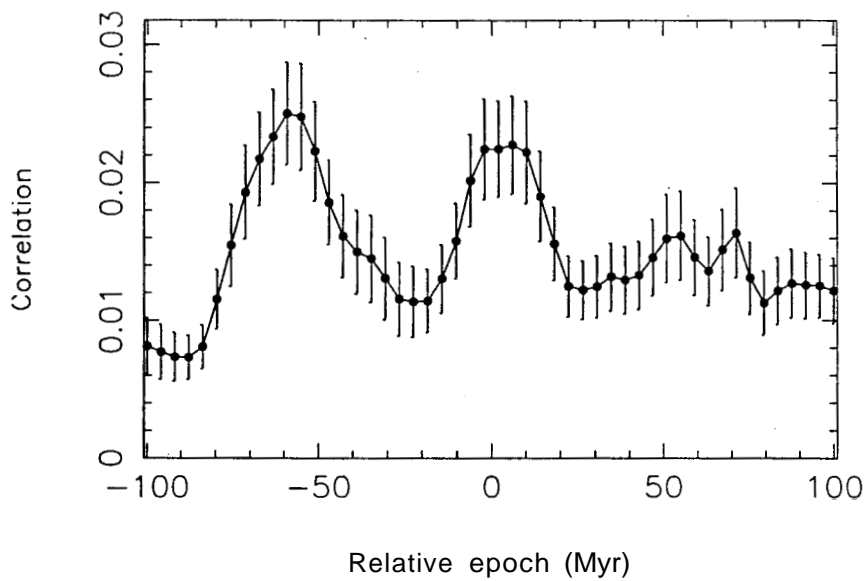


Figure 4.4: Plot of the correlation of the mass distribution in the spiral arms with the present pulsar distribution at various epochs. This plot corresponds to **a** corotation resonance radius of 14 kpc. The error bars indicate 1  $\sigma$  deviation on either side. The locations of the peaks of the correlation correspond to an epoch which is 60 Myr ago, and the present epoch.

of the spiral arms traced by the present distribution of pulsars. The possible reasons for the peak at the present epoch will be discussed in section 4.5.

The pulsars whose fields are in the range  $10^{10.5} - 10^{11.5}$  G are neglected from this analysis for they are believed to be recycled pulsars from intermediate mass range binaries (see chapter 2 of this thesis, and Deshpande *et al.* 1995).

### 4.3.1 Modified $d_{\min}$ distribution

As mentioned earlier, the scale factor is the ratio of the true number of pulsars in the Galaxy to the observed number. If the Galaxy is rotated back to the epoch where the correlation is maximum ( $-60$  Myr), one expects to find the distribution of  $d_{\min}$  with respect to the scale factors  $\mathcal{S}(R, \phi)$  symmetric and centred around zero  $d_{\min}$ . This is one of the necessary conditions to check the computation of scale factors. Figure 4.5 shows this distribution after rotating the Galaxy in time by  $-60$  Myr. This distribution is much more symmetric than the one shown in figure 4.2. It is also seen that this modified  $d_{\min}$  distribution is more compact and symmetric than similar distributions computed for various other epochs.

### 4.3.2 Minimum mass for neutron star formation

As mentioned earlier, the correlation between the past spiral structure and the distribution of pulsars in the Galaxy was conjectured by Blaauw in 1985. If the progenitors of pulsars are massive stars (say,  $\gtrsim 15M_{\odot}$ ), one would expect a correlation of the pulsar distribution with the spiral pattern at almost present epoch, for massive stars do not live longer. In other words, the time scale for the spiral arms to significantly overtake the matter distribution in the Galaxy may be much more than the lifetime of massive stars. However, what Blaauw found was quite different. His analysis can be summarised as follows. In his work

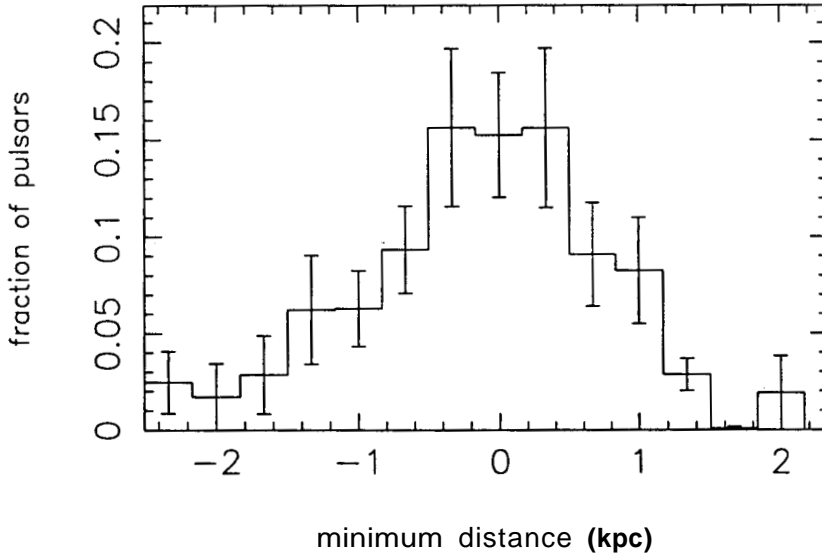


Figure 4.5: Distribution of  $d_{\min}$  after compensating for selection effects. Y-axis gives the true number of pulsars (after scaling the observed number of pulsars by appropriate scale factors as a function of position in the Galaxy). This distribution is produced after rotating the Galaxy by  $-60$  Myr. The error bars indicate  $1\sigma$  deviation on either side.

Blaauw restricted himself to the observed sample of pulsars whose distances from the Sun projected onto the plane of the Galaxy are less than 0.5 kpc. After calculating the death rate of massive OB stars in the local OB associations he came to the conclusion that the local pulsar population cannot be replenished by the OB associations alone. The field stars must therefore make a significant contribution. While trying to match the local pulsar birth rate to the death rate of local massive stars, he concluded that the overwhelming majority of the pulsar progenitors should correspond to relatively less massive stars in the range of  $6 - 10M_{\odot}$ . Based on more limited data set Gunn & Ostriker (1970) had also come to the same conclusion. If this is true, then since the less massive stars live longer, an equally important corollary is that 'pulsars, on the Galactic scale, are tracers of past spiral structure (20 – 50 Myr ago) rather than of active spiral structure' (Blaauw 1985).

The correlation analysis described in section 4.3 confirms this prescient conjecture. As can be seen from our correlation curve in figure 4.4, the correlation peaks at  $-60$  Myr. This means that the epoch of the formation of stars which gave birth to most of the present pulsars is  $\approx 60$  Myr. To the first approximation this time scale is the sum of the life time of the progenitors of pulsars and the average age of the present population of pulsars. A weighted average of characteristic ages with the scale factors gives the average age of the pulsar population.

$$\langle \tau \rangle = \frac{\sum_{i=1}^{N'_{\text{psr}}} S_i(R, \phi) \tau_i}{\sum_{i=1}^{N'_{\text{psr}}} S_i(R, \phi)} \quad (4.4)$$

Here,  $\tau_i$  is the characteristic age (defined as  $P/2\dot{P}$ ) of  $i^{\text{th}}$  pulsar and  $S_i(R, \phi)$  is the corresponding scale factor.  $N'_{\text{psr}}$  is the number of pulsars confined to the regions where the model density is non-zero at the relative epoch of  $-60$  Myr.

This average turns out to be  $(10 \pm 2)$  Myr. Therefore the average age of the progenitors is about 50 Myr, which corresponds to a  $7M_{\odot}$  star (see Schaller *et al.* 1992). Therefore, one may conclude that all stars which are more massive than about  $7M_{\odot}$  would result in producing neutron stars. It is worth mentioning here that when pulsars in different average age ranges were selected, the correlation peak (corresponding to the past epoch) was seen to shift systematically implying a roughly constant age for the progenitor stars.

### 4.3.3 Resonance radii of the Galaxy

As mentioned earlier, figure 4.4 shows a peak corresponding to a relative epoch of  $-60$  Myr, for an assumed corotation resonance radius of **14** kpc. This correlation analysis was repeated for various values of corotation radii. Since almost all pulsars are confined to within a galactocentric distance of about **13** kpc, naturally the analysis is not very sensitive to variation of values of the corotation radius beyond a value of about **12** kpc. However, for values of  $R_c$  less than **12** kpc, the correlation peak was seen to broaden and shift rapidly to earlier epochs disappearing completely for  $R_c$  below about 10 kpc. This is consistent with the kinematic models of the Galaxy based on neutral hydrogen observations, where one finds that the model fits rather well with observations with the assumed  $R_c = \mathbf{14}$  kpc (Burton 1971).

The resonance radii (Inner and Outer Lindblad resonance radii and the corotation resonance radius) play a major role in the study of spiral patterns and bars in galaxies. The relation between the resonance radii is as given below (see Binney & Tremaine 1987).

$$\omega_{\text{ILR}} = \omega_p + \kappa/2; \quad \omega_{\text{OLR}} = \omega_p - \kappa/2 \quad (4.5)$$

Here,  $\omega_p$  is the angular velocity of the spiral pattern,  $\kappa$  is the epicyclic frequency.  $\omega_{\text{ILR}}$  is the angular velocity corresponding to the Inner Lindblad Radius, and  $\omega_{\text{OLR}}$  is the angular velocity corresponding to the Outer Lindblad Radius. For a flat rotation curve,  $\kappa = \sqrt{2}\omega$ . Thus, for a given value of the corotation radius  $R_c$ , the inner and the outer Lindblad Resonance Radii would be  $0.3R_c$  and  $1.7R_c$  respectively. Since there is clear evidence for the presence of spiral arms beyond  $R = 4$  kpc, the inner Lindblad resonance radius is unlikely to be greater than 4 kpc. This would suggest a corotation radius  $\leq 13$  kpc, consistent with what is seen in this analysis viz.  $12 \leq R_c \leq 15$  kpc. Thus, the estimate of the Inner and the Outer Lindblad Resonance Radii are  $3.5 - 4$  kpc and  $21 - 25$  kpc respectively. It is worth mentioning here that Mulder and Liem (1986) estimate  $R_c$  to be  $\sim 8.5$  kpc from their global gas dynamical model.

#### 4.3.4 Significance of the correlation maximum

A small Monte Carlo simulation was done to test the statistical significance of the correlation shown in figure 4.4. The procedure adopted was the following. (1) Every pulsar was assigned the longitude of some other pulsar, keeping their original distances the same, (2) scale factors corresponding to their new positions in the Galaxy were computed, (3) this new set of parameters were used to compute the correlation as a function of the relative epoch, and the value of the maximum correlation was noted.

The above given procedure (step 1–3) was repeated thirty thousand times. Then, from the distribution of maxima of correlations, the statistical significance of the feature at  $-60$  Myr is 99.95%. After scrambling the longitudes, a further test was made by also varying the distances by about 30% (rms), which showed an even higher significance for the correlation maximum found at  $-60$  Myr.

The significance of the feature at the present epoch (zero Myr) was also tested in a similar manner but with maxima searched over an epoch range of  $-2.5$  Myr to  $25$  Myr. This significance turned out to be about  $93.3\%$ , which is rather poor.

## 4.4 Limits on space velocities of pulsars

As explained in section 4.3.1 after correcting for selection effects the  $d_{\min}$  distribution was modified. The modified  $d_{\min}$  distribution is plotted in figure 4.5. If one assumed that the spread in this modified  $d_{\min}$  distribution is caused only by the spatial velocities of pulsars, then by studying the width of the modified  $d_{\min}$  distribution it is possible to estimate some useful quantities related to the spatial velocities of pulsars.

For this purpose, a subset of the sample set was chosen on the basis of the distance from the nearest spiral arm; *i.e.*, at the relative epoch of  $-60$  Myr (when the correlation is maximum) the pulsars which are within a distance of  $|d_{\min}| \leq 0.9$  kpc are included. This is because, as mentioned earlier, the mass distribution perpendicular to the spiral arm is a Gaussian with  $a = 0.3$  kpc. Also, an age cutoff of  $10$  Myr was chosen. These cutoffs were to make sure that only those pulsars which contribute to the correlation peak is chosen for this analysis. For each pulsar thus selected a projected velocity can be computed by dividing its  $d_{\min}$  value by its characteristic age.

The relation between the projected velocity distribution and the real velocity distribution can be derived on the basis of the following arguments. If pulsars are distributed following a real velocity distribution  $P(v)$  and evolved for a fixed age  $\tau$ , the number of pulsars in a unit volume at a distance  $(vt)$  is proportional to  $P(v)/(vt)^2$ . Pulsars in a shell of radius  $(v_0\tau)$  contribute uniformly to all projected



velocities in the range zero to  $v_o$ . In general the distribution of projected velocities can be expressed as,

$$P_p(v_p) = \int_{v_p}^{\infty} \frac{P(v)}{v} dv \quad (4.6)$$

It must be noted here that since the projected velocity is defined in the plane of the Galaxy, this procedure is unaffected by the height of the birth places above the plane, and by the accelerations normal to the plane.

#### 4.4.1 Accounting for distance uncertainties

The value of  $d_{\min}$  of a given pulsar depends on its location in the Galaxy. Since the location of any pulsar in the Galaxy depends on the distance model used, it is essential to estimate the effect of uncertainties in the distance model. In their paper Taylor & Cordes (1993) have estimated the average uncertainty in the distance to be about 25%. If the range of  $d_{\min}$  values is comparable to the errors in distance to pulsars from the Sun, then the results regarding the velocities of pulsars will be seriously affected. In order to independently estimate the fractional error in the distance model, the following procedure was used.

An error of  $x\%$  was added to the distance and the distribution of correlation maxima was computed by a Monte Carlo simulation. For  $x$  small compared to the intrinsic error  $x_o$  in the distance model, this would make little difference. The computed distribution will be highly peaked around  $C_o$  (maximum correlation in figure 4.4). For  $x$  large compared to  $x_o$  our ensemble will behave like the one in which the true distances have errors  $x \gg x_o$ . In this case the distribution of maxima will typically be less than  $C_o$ . The value of  $x_o$  was estimated by the value of  $x$  for which the significance of  $C_o$  saturates. It was found that the significance level was about 40% when negligible error was introduced, and it saturated at

about 80% when about 20% error was introduced. Incidentally, the value derived here matches very well with the value given by Taylor & Cordes (1993).

To minimise the effect due to this error in distance, the following procedure was adopted. For every pulsar the distance was varied by 20% (rms) and the variance in the minimum distance  $\sigma_{d_{\min}}$  was computed. The error in the projected velocity then can be computed as  $\Delta v = \sigma_{d_{\min}}/\tau_{ch}$ . To reduce the contribution from pulsars with large values of  $\Delta v$  a weighting function was used, which is given by,

$$w_d = \exp \left[ - \left( \frac{\sigma_{d_{\min}}}{\tau_{ch} \Delta v_{\max}} \right)^2 \right] \quad (4.7)$$

Here,  $\Delta v_{\max}$  was chosen arbitrarily to be 40 km/sec. To demonstrate how important it is to apply the distance weighting function to get reliable estimate of velocity parameters, the resultant spread in the velocity distribution caused merely due to the distance uncertainties as a function of the tolerance level ( $\Delta v_{\max}$ ) was estimated. For arbitrarily large  $\Delta v_{\max}$  (which is the case where  $w_d$  is more or less the same for all pulsars), this resultant rms spread turns out to be about 500 km/sec (for about 20% error in distances), emphasising the need for the explicit weighting in distance. For  $\Delta v_{\max} = 40$  km/sec. for the tolerance level, the spread came down to **42** km/sec. Therefore as long as the mean velocity is greater than  $\approx 80$  km/sec., it may not be seriously affected by the distance uncertainties.

#### 4.4.2 Aliasing due to finite interarm spacing

If the velocity of a pulsar is greater than  $(D/2\tau)$ , where  $D$  is the interarm spacing, the velocity gets aliased with the contributions in the range zero to  $(D/2\tau)$ . This effect, as one can expect, is quite serious in the regions where the interarm spacing is small. This aliasing can lead to the underestimation of mean velocity. This

effect can be overcome with the following weighting function.

$$\begin{aligned} W_a &= \left[ \frac{D}{D_o} \right]^a, & D < D_o \\ W_a &= 1 & D \geq D_o \end{aligned} \quad (4.8)$$

Here,  $D$  is the interarm spacing at the location of the pulsar, and  $a$  is the weighting exponent. The value of  $D_o$  is chosen to be 4 kpc. In the selected set of samples most of the pulsars which would be seriously affected by aliasing are also the ones weighted down by distance weighting factor (equation 4.7). Therefore the results were not very sensitive to the weighting function for aliasing.

### 4.4.3 Estimation of average velocities

The average value of  $d_{\min}$  and age turn out to be  $(0.3 \pm 0.07)$  kpc, and  $(2.8 \pm 0.7)$  Myr, respectively. A simple minded mean projected velocity estimate from these two values turns out to be  $(105 \pm 35)$  km/sec. If one assumes a Maxwellian type of distribution for speed, the implied mean velocity is about  $(200 \pm 70)$  km/sec. The other way to calculate this number would be to calculate the mean of the projected velocities of each pulsar (calculated from its characteristic age and  $d_{\min}$ ). This value turns out to be  $(80 \pm 20)$  km/sec., implying a mean velocity of about  $(160 \pm 40)$  km/sec. Although, in principle, one should be able to fit a function to get the distribution of projected velocities (which, in turn, will give the velocity distribution of pulsars), due to statistical noise it turns out to be impossible. Also, for this exercise only those pulsars which fall within  $d_{\min} = 0.9$  kpc was included. Therefore this analysis is not sensitive to velocities  $\gtrsim 400$  km/sec.

## 4.5 Discussion

The Initial Mass Function of stars in the Galaxy is quite steep:  $\psi(M) \propto M^{-2.7}$  (Salpeter 1955; Scalo 1986). Hence, most of the pulsars are born from stars of mass close to the threshold mass for neutron star formation. Therefore the epoch of maximum correlation should correspond to the life time of the progenitors close to the threshold mass. Lesser correlation is expected from pulsars born from progenitors with masses larger than the threshold mass. Also, this will be at epochs more recent than the epoch of maximum correlation consistent with the evolutionary time scales of the more massive progenitors. Indeed, such a tail may be seen in figure 4.4.

While associating the inferred progenitor star lifetime of 50 Myr with a mass of the progenitors ( $\sim 7M_{\odot}$ ), it is assumed that the progenitors are single stars. The recycled pulsars from binary systems will not affect this interpretation for the following reason. The time taken from the binary formation to the release of the recycled pulsar may be longer by as much as a factor of two or more (depending on the mass-ratio) compared to the solitary progenitors, for recycled pulsars are produced only at the end of the second explosion of the binary. However, the progenitors from binary systems will contribute to the correlation at epochs spread over a large range depending upon the mass of the companion. Hence one may conclude that the correlation peak must be essentially due to pulsars from solitary progenitors.

The formal uncertainty in the epoch of maximum correlation derived from the statistical errors in the correlation turns out to be  $\pm 10$  Myr. However, a good fraction of this can be attributed to a genuine width of a correlation that one would obtain for a fixed mass of progenitors (for example, if stars of the limiting

mass are born over a region of width  $\approx 100$  pc along the spiral arms, one would see the correlation width to be  $\approx 16$  Myr). Hence one may conclude that the uncertainties are small enough to constrain the threshold mass of the progenitors to be  $\sim 7M_{\odot}$ .

The correlation between the pulsar distribution and the spiral pattern as a function of azimuthal rotation is sensitive in the regions where the arms are not azimuthal, as also in the regions away from the corotation resonance radius. The pulsars in the region of corotation and the regions where the spiral arms are azimuthal contribute a non-varying component of the correlation.

While computing the correlations at various epochs only the present galactocentric radius was used since the galactocentric distances of pulsars at the earlier epochs can not be guessed. However, the error introduced due to this is expected to get averaged out as the number of samples is sufficiently large.

The origin of the feature at zero Myr (see figure 4.4) needs some discussion. One possible way this feature can arise is due to the overestimation of the number density of electrons in the arm component of the electron density model. This is because an increase in the number density of the ~~arm~~ component results in an artificial clustering of pulsars close to the arms. Also, if one looks at the geometry of the spiral arms in the Galaxy it appears as though the pulsars on (or close to) any given arm will get transferred to the nearby arm after going through roughly  $90^{\circ}$  degrees (which happens to be roughly 60 Myr for bodies close to the solar circle). Therefore, if one attributes correlation at the present epoch (zero Myr) because of the artificial clustering of pulsars due to the overestimation of the arm density, the feature at  $-60$  hlyr may also be due to the same reason. However, if one looks at figure 4.6 one can see that many of the pulsars which fall on the spiral arms (which are rotated by  $-60$  Myr) are not the pulsars concentrated

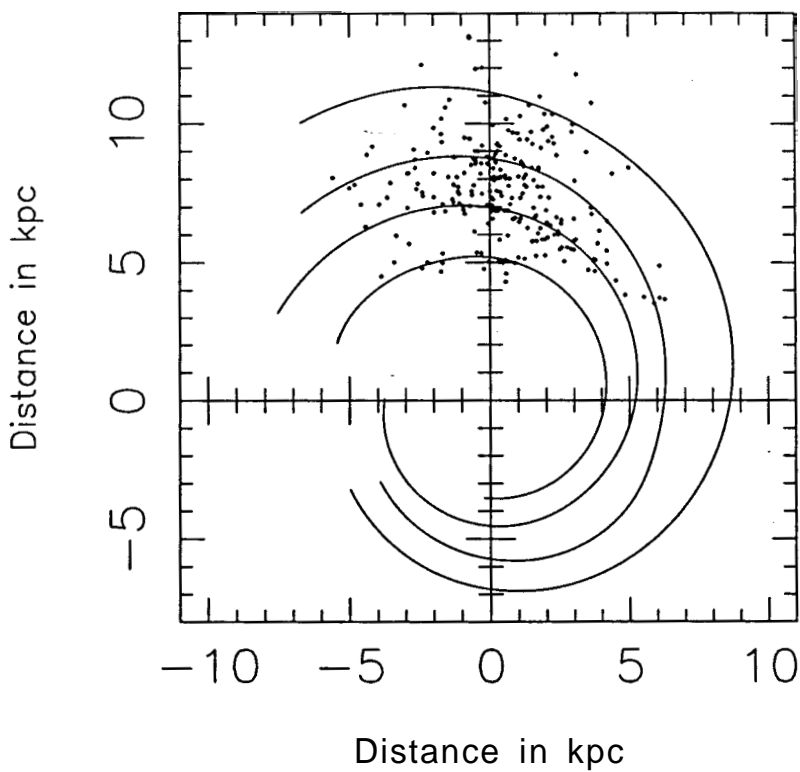


Figure 4.6: The spiral arms of the Galaxy after getting rotated by  $-60$  Myr. Though the spiral pattern is supposed to rotate like a rigid pattern, to have a clear idea of the location of spiral arms with respect to the distribution of pulsars, the distribution of pulsars is taken to be rigid, and the spiral pattern is rotated by  $-60$  Myr.

near the spiral arms at zero Myr. To prove this quantitatively a few tests were conducted and the results can be summarised as follows.

To check how sensitive the correlation diagram is to a change in the arm density, the arm density was varied by some fraction (keeping the total electron content in the Galaxy approximately the same. *i.e.*, the electron density of the disk component of the model was correspondingly changed to make up for the change in the arm component). When the arm density was decreased, the height of the component at zero Myr decreased, whereas it did not change appreciably at  $-60$  Myr. Similarly, when the arm density was increased, the zero Myr feature increased in its height. This gives us some confidence to say that the feature at  $-60$  Myr may be real. For example, even when the arm density was decreased to very low values the correlation at  $-60$  Myr did not vanish. Therefore we conclude that the zero Myr feature may be due to a combination of the overestimation of the number density of the arm component, and the geometry of the spiral arms of the Galaxy.

While estimating the average velocity of pulsars, the spread in  $d_{\min}$  due to the width of the spiral arms and the progenitor velocities are neglected. Since the velocities of pulsars are in general believed to be much larger than the velocities of massive stars in the Galaxy (see Lyne *et al.* 1982; Bailes *et al.* 1990; Harrison *et al.* 1993), one expects the former to dominate the spread in the  $d_{\min}$  distribution. Also, while deriving the average velocity pulsars with  $\log B < 11.5$  have also been neglected since they would introduce a systematic bias towards low velocities. This is because these pulsars are identified to be the recycled pulsars from intermediate mass range binaries (Bailes 1989; Deshpande *et al.* 1995), and they are shown to have relatively low velocities.

The velocities inferred from VLBI proper motion measurements are on the

average much higher than mean velocity of  $160 - 200$  km/sec as estimated by us in section 4.4. If the large proper motions are considered as from the tail of the velocity distribution, then there should be a considerable number of low velocity pulsars for which such proper motion measurements are yet to be done. This is not very surprising since the proper motion measurement techniques tend to select against low velocity and far away pulsars.

As mentioned in section 4.4.3 this analysis is not sensitive to velocities greater than  $\approx 400$  km/sec.

From an independent analysis of pulsar population, Narayan & Ostriker (1990) have argued for two distinct distributions for pulsar velocities. They estimate 50 and 150 km/sec. as the mean one dimensional velocities for their low and high velocity populations, respectively, with roughly half of the pulsar population in each distribution. This would imply a mean velocity of the population in agreement with our estimate ( $160 - 200$  km/sec.).

The main results of this chapter can be summarised as follows.

- The corotation resonance radius of the Galaxy is estimated to be  $(13 \pm 1.5)$  kpc. Assuming a flat rotation curve for the Galaxy, the other two resonance radii (the inner and the outer Lindblad resonance radii) are estimated to be in the range  $3.6 - 4.5$  kpc and  $21.4 - 25.5$  kpc respectively.
- The correlation between the present position of pulsars and the location of the spiral pattern in the past suggests that the age of the progenitors of the present pulsar population, on the average, are 50 Myr or so. This age corresponds to  $\approx 7M_{\odot}$ .
- The global mean of pulsar velocities is estimated to be in the range  $160 - 200$  km/sec.